Thermal transport and fire retardance properties of cellular metals

T. J. Lu, C. Chen
Cambridge University Engineering Department, Cambridge CB2 1PZ, UK

Abstract

The apparent thermal conductivities of two-dimensional foams having a variety of cellular microstructures are calculated. These include regular honeycombs, Voronoi structures and Johnson-Mehl models. The effects of several types of geometric imperfection are studied by using analytical as well as finite element methods. The coupling of solid conduction with thermal radiation is dealt with by using the method of finite elements. These results are then applied to solve the transient temperature field of a cellular metal plate subjected to a sudden introduction of a high temperature source of heat such as fire. The factors which dictate the thermal and structural fire retardance of cellular metallic foams are identified.

1 Introduction

In the absence of forced convection, the transport of heat across a cellular metal foam having either open or closed cells is dominated by conduction along the solid cell walls and thermal radiation amongst the cell walls, and can be described in terms of the relative amounts and arrangement of its constituents. The apparent thermal conductivity k of a low-density metal foam due to conductive heat transfer alone is related linearly to its relative density ρ -- defined as the ratio of the density of the foam to that of the solid of which the foam is made -- according to

$$k = \zeta \rho k_s \tag{1}$$

where k_s is the solid conductivity and the efficiency coefficient ζ accounts for the tortuous shape of the cell walls. The proportionality coefficient ζ is sensitive to changes in morphological details and so is expected to vary from one cellular structure to another. As such, it is also dependent upon the various types of geometric imperfection commonly found in commercial metal foams. Typical morphological defects include Plateau borders, broken cell walls, missing cells, cell-wall misalignments, cell size variations and inclusions. These defects are found to be responsible for the significant knock-down of the hydrostatic yield strength of metal foams [1]; their effects on thermal transport properties are studied here using analytical as well as numerical approaches. The coupling of conductive and radiative heat transfer in regular honeycombs is considered. Finally, the one-dimensional transient heat transfer problem of a finite plate the surface of which is suddenly exposed to fire is solved to analyse the fire retardance properties of metallic foams.

2 Conductive heat transfer

The apparent thermal conductivities are calculated for several two-dimensional linear networks having different cell shape and node connectivities. These include regular hexagonal honeycombs and lattices with equilateral triangle packing, square packing or packing of circles (Fig. 1), Voronoi structures, and Johnson-Mehl models (Fig. 2). The lattice structures considered are either isotropic or orthotropic, with k denoting the apparent conductivity in the principal direction. The calculated results are summarised in Table 1. In general, a higher connectivity results in a lower conductivity, and the conductivity of a regular honeycomb (connectivity 3) provides an upper bound for the 2-D foams considered in this paper.

A variety of processing induced morphological imperfections are known to degrade the mechanical properties of metallic foams [1]. The measured thermal conductivities of cellular foams are usually smaller than those predicted, and this has also been attributed to the presence of imperfections. Here, for simplicity, the effect of different types of geometric imperfection is studied separately. A

J. Banhart, M.F. Ashby, N.A. Fleck: *Metal Foams and Porous Metal Structures.* © MIT Verlag (1999)

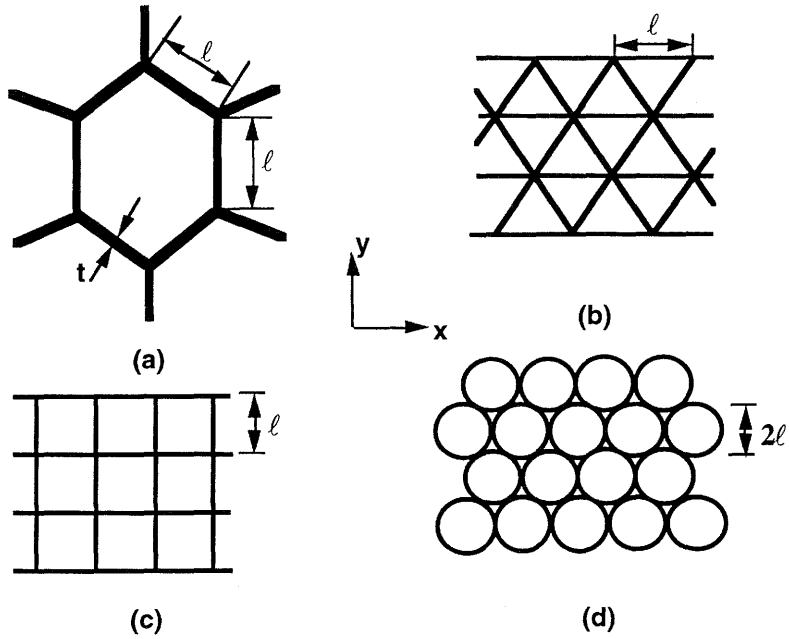

Fig. 1 Two-dimensional lattices: (a) regular hexagonal honeycomb, (b) packing of equilateral triangles (c) packing of squares, (d) closely-packed circles.

Table 1. Thermal conductivities of two-dimensional cellular solids.

Cell shape	Equilateral triangle	Square	Circle	Regular hexagon	Γ – Voronoi	δ – Voronoi	Johnson-Mehl
Connectivity	6	4	4	3	3	3	3
$k / \rho k_s$	1/2	1/2	$9/2\pi^2$	1/2	0.433	0.477	0.393

simple analytical model is developed for one type of periodic imperfections, the Plateau borders, and it is established that Plateau borders decrease the conductivities, especially those of low-density foams where the reduction can be as high as 50 percent. The effects of four different types of random geometric imperfection -- cell-wall misalignments, fractured cell walls, missing cells, and solid inclusions -- are studied for a regular hexagonal honeycomb by using the finite element code ABAQUS. Finite element models are first developed for a perfect honeycomb. The cell-wall misalignments are then introduced to by randomly displacing its joint nodes, i.e., the nodes met simultaneously by three cell walls, according to

$$\begin{aligned} x'_k &= x_k + \alpha l \cos\phi \\ y'_k &= y_k + \alpha l \sin\phi \end{aligned} \tag{2}$$

where (x_k, y_k) and (x'_k, y'_k) are the co-ordinates of the original and displaced joint nodes, l is the cell wall length, α is a scalar measure of the misalignments, and ϕ is a random angle between the x-axis and the line connecting the original and displaced joint nodes. To simulate fractured cell-walls commonly found in commercial Al foams, a given fraction of the cell walls are removed randomly from an initially perfect honeycomb. Missing cells are introduced by deleting one or more triangular joints. To model high relative density domains, selected cells are filled with solid inclusions made of the same material as that of cell walls. In the finite element analysis, each cell wall is modelled by 2 beam elements; the relative density of the model foam is changed by

changing the cell wall thickness. The total degrees of freedom in a typical finite element model is in the range 5,000 to 15,000, depending on the total number of cells used in the representative cell.

It is found that cell wall misalignments only have a relatively small effect on conductivity. Randomly distributed broken cell walls, on the other hand, have a relatively large knock-down effect on conductivity. With f_b denoting the number fraction of broken cell walls, the results can be approximated by

$$k/k_0 = 1-(10/3)f_b \tag{2}$$

where $k_0 = (1/2)\rho k_s$. Like cell wall misalignments, missing cells decreases slightly the conductivity which can be described by

$$k/k_0 = 1-(5/3)f_m \tag{3}$$

where f_m is the volume fraction of cells that are missing. Solid inclusions tend to slightly increase the conductivity; however, when the increase in relative density due to inclusions is taken into account, the results are similar to those for Plateau borders.

2.1 Voronoi structures and Johnson-Mehl models

To create a 2-D Voronoi diagram for finite element calculations, randomly generated nucleation points are placed in a 2-dimensional domain according to an assumed distribution function. The domain is then divided into Voronoi polygons by drawing lines from each point to the nearest-neighbouring points, with normals drawn to bisect these lines. The area surrounding each generation point enclosed by the normals constitutes the Voronoi cell, typically a polygon with 4 to 8 sides. If a Voronoi diagram is generated without placing any constraints on the minimum distance between neighbouring random points, the resulting cell size distribution follows essentially the Γ – distribution. If, however, a minimum allowable distance between two neighbouring nuclei is specified, the resulting Voronoi diagram has nearly uniform cell size distribution, i.e., the δ – distribution. Both types of cell size distribution are modelled to quantify their effects on transport properties of cellular foams. The results are presented in Table 1 to compare with those for honeycombs. In the absence of other types of imperfection, Γ – distributed Voronoi structures have the lowest thermal conductivity amongst the three honeycombs studied, with $k/k_0 = 0.866$. For δ – distributed Voronoi structures, $k/k_0 = 0.954$, which is about 5% smaller than that of a perfect honeycomb ($k/k_0 = 1.0$). The conductivity of a Voronoi structure is reduced further by broken cell walls and the behaviour is qualitatively similar to that of Eq. (2) for a regular honeycomb. These results remain unchanged if new Voronoi structures generated using different sets of random points are used in the finite element calculation.

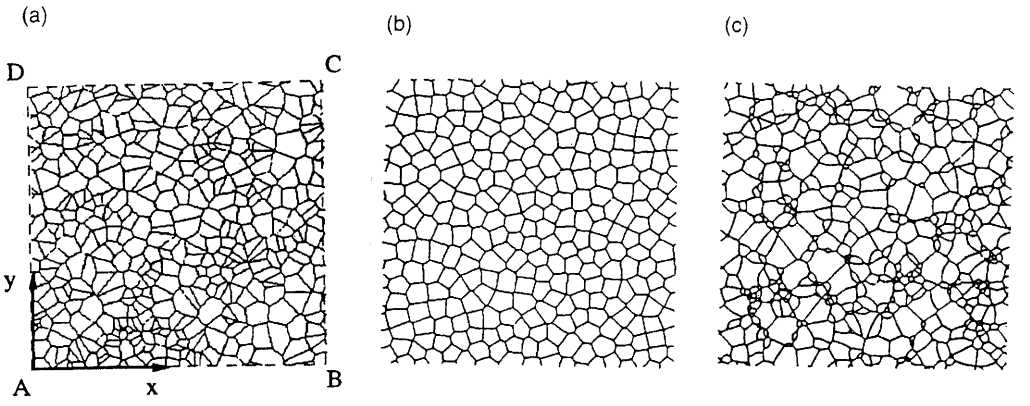

Fig. 2 Typical finite element mesh for a periodic honeycomb with (a) Γ – distributed cells, (b) δ – distributed cells, and (c) Johnson-Mehl cells. Beam elements are used.

In contrast to the simultaneous nucleation of bubbles in a Voronoi structure, the nucleation in a Johnson-Mehl model is continuous, following the Poisson process. Here, the nuclei of bubbles appear randomly *both* in space and in time, and grow at a constant rate. The selection of a nucleation site is random. It is eliminated from the nucleation sequence if it falls into the area covered by an existing bubble. Compared to Voronoi cells bounded by straight lines and having three or more distinct sides, the Johnson-Mehl structure is more complex. The surface of impingement between two neighbouring nuclei forms a hyperboloid of revolution, being symmetric relative to the line joining the two nuclei and convex toward to the nucleus formed first. Thus, the cells in a Johnson-Mehl structure are irregular with curved cell walls, some of which being two-sided and one-sided. These features resemble the microstructures of a number of metals (e.g., recrystallised iron) and, at least partially, those of Al alloy foams. In the absence of broken cell walls, the calculated conductivity of a Johnson-Mehl structure is about 21% smaller than that of a perfect honeycomb at the same relative density level, i.e., $k/k_0 = 0.786$ (Table 1). It has been established that this result holds for Johnson-Mehl models generated with different seeds of random points.

3 Coupling of conductive and radiative heat transfer

In the presence of radiation, Eq. (1) for the apparent thermal conductivity can be modified as

$$k = k_c + k_r = \zeta k_s \rho + \xi \varepsilon \sigma T_m^3 l \tag{4}$$

where k_c and k_r are the apparent thermal conductivities due to solid conduction and radiation, respectively, ε is the emissivity of the cell wall surface, l is the cell size, σ is the Stefan-Boltzmann constant, T_m is the mean temperature of the foam, and ξ is a dimensionless parameter. It is expected that k_r is a function of temperature, foam thickness, cell size and relative density. Because radiation is a highly nonlinear process, the effect of radiative heat transfer on the transport of heat in a two-dimensional regular hexagonal honeycomb is studied here with the method of finite elements. The region enclosed by the walls of a hexagonal cell is modelled as a cavity; each cell wall is discretised into 32 solid elements (8 along the length and 4 across the thickness). Each element is assumed to be isothermal and to have a uniform emissivity ε that is independent of temperature. In addition, grey body radiation (ε independent of the wavelength of propagation of the radiation) and diffusive (nondirectional) reflection is assumed, and attenuation of the radiation in the cavity medium is ignored.

In the finite element model, each cavity (cell) is made up of a collection of N element faces (facets) corresponding to the finite element discretisation around the cavity. Let A_i $(i = 1,2,...,N)$ denote the surface area of the ith facet and T_i its *average* temperature, the radiation flux into facet i can be written as

$$q_i^r = \frac{\sigma \varepsilon^2}{A_i} \sum_{j=1}^{N} \sum_{k=1}^{N} F_{ik} C_{kj}^{-1} \left(T_j^4 - T_i^4 \right), \quad i = 1,2,...,N \tag{5}$$

where $C_{ij} = \delta_{ij} - (1-\varepsilon) F_{ij} / A_i$ (no summation), δ_{ij} is the Kronecker delta, and F_{ij} is the geometrical view factor between two facets A_i and A_j:

$$F_{ij} = \int_{A_i} \int_{A_j} \frac{\cos\phi_i \cos\phi_j}{\pi R^2} dA_i dA_j \tag{6}$$

Here, R is the distance between the two facets and ϕ_i, ϕ_j are the angles between R and the normals to the surfaces of the facets. An automatic viewfactor calculation capability is offered by ABAQUS. In the limiting case of blackbody radiation ($\varepsilon = 1$), (30) reduces to

$$q_i^r = \frac{\sigma}{A_i} \sum_{j=1}^{N} F_{ij} \left(T_j^4 - T_i^4 \right), \quad i = 1,2,...,N \tag{7}$$

A spatial interpolation technique is used to calculate the radiation flux q_i^r, the variables being the temperatures of the nodes on the cavity surface.

The apparent conductivity of a regular honeycomb due to radiative heat transfer alone, $k_r \equiv k - k_0$ where $k_0 = k_c = (1/2)\rho k_s$ is the apparent conductivity due to solid conduction, is found to be proportional to ε and T_m^3, in accordance with (4). In addition, it has been verified that, when $\varepsilon = 0$ (no radiation), the finite element model reproduces the result $k = k_0 = (1/2)\rho k_s$. When $k_s > 20$ W/(m · K), the transport of heat is dominated by solid conduction ($k_r << k_c$) so that the effect of radiation can be ignored. For insulation materials where k_s is typically less than 1 W/(m · K), radiation heat transfer is no longer negligible as it contributes more than 50% of the total heat being transported even at relatively low temperatures ($T_2 \sim 40°C$). For metallic foams where $k_s > 100$ W/(m · K), the result that $k_r / k_0 < 0.1$ holds in the entire range of temperature considered ($30°C < T_2 < 530°C$). The cell wall length l also affects the radiative conductivity, with k_r increasing as l increases. At high temperatures ($T_2 \sim 500°C$), however, k_r appears to attain an asymptotic value for relatively large cells ($l \sim 4$mm). Finally, thermal radiation is seen to become increasingly dominant as the foam relative density ρ decreases, particularly so if k_s is small (< 1 W/(m · K)).

4 Fire retardance of metallic foams

A simple heat transfer model is developed below to explore the various factors that dictate the capability of a metallic foam to resist fire. Thermal failure occurs when the insulating capability of the specimen is lost. Consider a cellular metal plate, thickness L and initial temperature T_0, the front surface of which is suddenly raised to temperature at time t=0 (Fig. 3). It is assumed that the plate thickness L is small compared with its other dimensions such that the loss of heat from the sides is negligible, and that the area of the plate is sufficiently large to allow the heat being conducted perpendicularly across the plate thickness. A portion of the heat is consumed on raising the temperature of the plate, the rest being lost to the environment via the rear surface of the plate at x=L. Under these assumptions, an one-dimensional analysis of the problem is appropriate and the temperature of the plate may be expressed as T=T(x,t). With κ denoting the thermal diffusivity of the plate in the x-direction, the one-dimensional conduction of heat is governed by

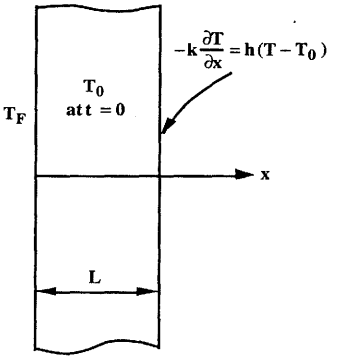

Fig. 3 A panel of finite thickness with specified thermal boundary conditions.

$$\frac{\partial^2 T}{\partial x^2} = \frac{1}{\kappa}\frac{\partial T}{\partial t} \tag{8}$$

where constant thermophysical properties are assumed. The initial and boundary conditions appropriate for the problem are

$$T(x,0) = T_0, \quad \text{when } t = 0; \text{ for } x \geq 0 \tag{9}$$

$$T(0,t) = T_F, \quad \text{at } x = 0; \text{ for } t > 0 \tag{10}$$

In addition, heat transfer at the unexposed surface of the panel takes place by a combination of natural convection and radiation into a nonreflecting air mass of temperature T_0, with a constant coefficient h

$$-k\frac{\partial T}{\partial x} = h(T - T_0), \quad \text{at } x = L; \text{ for } t > 0 \tag{11}$$

where k is the thermal conductivity of the foam.

Use of the integral method results in the following approximate but simple solution

$$\frac{T(x,t)-T_0}{T_F-T_0}=\left(1-\frac{x}{\sqrt{10\kappa t}}\right)^2, \qquad \text{when} \quad 0\le t\le t_0$$

$$=\left(1-\frac{x}{L}\right)^2+\left(\frac{1+Bi(1-x/L)}{1+Bi}-\left(1-\frac{x}{L}\right)^2\right)\left\{1-e^{-\Phi^{-1}\frac{\kappa(t-t_0)}{L^2}}\right\}, \qquad (12)$$

$$\text{when} \quad t\ge t_0$$

where $t_0 = L^2/10\kappa$ is the penetration time of the applied heat to the rear surface of the plate at $x = L$, Bi is the Biot number defined as $Bi = hL/k$, and Φ is a function of the Biot number given by

$$\Phi(Bi)=\frac{4+Bi}{12(1+Bi)} \qquad (13)$$

In the limit $t\to\infty$, Eq.. (12) reduces to the limit

$$\frac{T^{\infty}(x)-T_0}{T_F-T_0}=\frac{1+Bi(1-x/L)}{1+Bi} \qquad (14)$$

where $T^{\infty}(x)$ is the steady-state temperature at an arbitrary location x.

4.1 Fire resistance parameters

Thermal fire resistance τ of a structural component is defined here as the time to failure by excessive heat transmission whereby it has lost its insulating capability. For a plane panel shown in Fig. 3, failure may be deemed to occur at the time when the temperature of its unexposed surface, T_B, reaches a critical value T_C (e.g., the melting temperature T_M). From (12), this can be readily calculated as

$$\tau=\frac{L^2}{\kappa}\left\{\frac{1}{10}-\Phi(Bi)\ln\left[1-\frac{T_C-T_0}{T_B^{\infty}-T_0}\right]\right\} \qquad (15)$$

where T_B^{∞} is the steady state limit of T_B, given by

$$T_B^{\infty}=T_0+\frac{T_F-T_0}{1+Bi} \qquad (16)$$

The thermal fire resistance τ is a strong function of the Biot number $Bi = hL/k$, increasing as the value of Bi increases. For a fixed Biot number, the fire resistance is infinite if the imposed fire temperature is smaller than a threshold value. Mathematically, this can be expressed as

$$\kappa\tau/L^2\to\infty \quad \text{when} \quad T_F<T_F^{th} \qquad (17)$$

where the threshold temperature is

$$T_F^{th}=T_C+(hL/k)(T_C-T_0) \qquad (18)$$

Acknowledgements

This work was supported by the EPSRC and by the ARPA/ONR MURI program on Ultralight Metal Structures (No. N00014-1-96-1028).

References

[1] C. Chen, T.J. Lu and N.A. Fleck, J. Mech. Phys. Solids (1999) in press.